

Received March 3, 2020, accepted May 14, 2020, date of publication May 18, 2020, date of current version June 2, 2020.

Digital Object Identifier 10.1109/ACCESS.2020.2995458

Soil Salinization Information in the Yellow River Delta Based on Feature Surface Models Using Landsat 8 OLI Data

BING GUO^{1,2,3,4,5}, WENQIAN ZANG⁴, AND RUI ZHANG⁶

¹School of Civil Architectural Engineering, Shandong University of Technology, Zibo 255000, China

²Key Laboratory of Digital Earth Science, Institute of Remote Sensing and Digital Earth, Chinese Academy of Sciences, Beijing 100101, China

³Key Laboratory of Geomatics and Digital Technology of Shandong Province, Qingdao 266590, China

⁴Aerospace Information Research Institute, Chinese Academy of Sciences, Beijing 100101, China

⁵Geomatics Technology and Application Key Laboratory of Qinghai Province, Xining 810001, China

⁶Land Satellite Remote Sensing Application Center, Ministry of Natural Resources, Beijing 100048, China

Corresponding authors: Wenqian Zang (zangwq@radi.ac.cn) and Rui Zhang (zhangrui@163.com)

This work was supported in part by the Open Research Fund of Key Laboratory of Digital Earth Science, Chinese Academy of Sciences under Grant 2019LDE006, in part by the Open Fund of Key Laboratory of Geomatics and Digital Technology of Shandong Province, and in part by the Geomatics Technology and Application key Laboratory of Qinghai Province under Grant QHDX-2019-04.


ABSTRACT Soil salinization as one of the major eco-environmental problems, has greatly restricted the regional development of Yellow River Delta. In this paper, five parameters that derived from Landsat images, including MSAVI, Albedo, SI, I_{Fe2O3} , and WI have been utilized to establish ten feature spaces, and four categories of salinization detection model have been proposed. After analysis and comparison of inversion accuracy, the three typical surface parameters, including SI ($R^2 = 0.85$), I_{Fe2O3} ($R^2 = 0.83$), and WI ($R^2 = 0.83$) are better indices to retrieve the salinization information and the WI-SI point to line (soil line) model ($R^2 = 0.88$), the Albedo-SI point to line (wet line) model ($R^2 = 0.87$) and the Albedo- I_{Fe2O3} point to point model ($R^2 = 0.86$) have better applicability to monitor the salinization condition in the Yellow River Delta. The research results can provide technical method reference for salinization monitoring of other regions.

INDEX TERMS Soil salinity, Albedo, Landsat 8 image, MSAVI, monitoring.

I. INTRODUCTION

Yellow River Delta has the most integrated new-born salinization system in China [1], [2]. It has prominent soil salinization and fragile ecological environment because of less precipitation, large evaporation, serious uneven drought and flood, and significant seasonal dry and wet alternation [2]–[4]. Soil salinization has critically restricted the development of regional agricultural economy in the Yellow River Delta [5]–[7]. Thus, it is urgent to obtain the soil salinization information, which can provide decision supports for the prevention and governances of soil salinization [2], [8]–[11].

Traditional studies on soil salinization are mostly based on field measurements, which are characterized by expensive cost, time-consuming and small spatial scale [1], [2], [12]–[16]. During the past decades, remote sensing and Geographic Information System technology have provided a fast and accurate new approach to obtain the salinization information of large-scale regions [2], [17]–[22].

The associate editor coordinating the review of this manuscript and approving it for publication was Le Hoang Son .

Scudiero *et al.* [23] applied the linear modeling of remote sensing vegetation indices to explore the potentials of assessing soil salinity. Ivushkin *et al.* [3] produced a global soil salinity map by combining thermal infrared images, soil texture data and field observations with machine learning method. Wang *et al.* [24] conducted the detailed comparison in monitoring salinization between Sentinel-2 MSI and Landsat 8 image and found that MSI image performed better than Landsat 8 image. In recent years, the feature space models that constructed by surface parameters have been applied to monitor the soil salinization [25], [26]. Wang *et al.* [10] utilized the biophysical parameters, such as vegetation coverage, soil moisture and surface evapotranspiration, to propose a “Triangle methods” to analyze the process of soil salinization. Ha *et al.* [4] constructed the SI-Albedo feature space model and found that the change of soil salinity and soil moisture content had significant relations with soil salinization. Ding *et al.* [27] had proposed the MSAVI-VI feature space model to detect the regional salinization information and found that there existed significant relationships between MWI index and surface soil salinity. Zhang *et al.* [28] had

explored the relationship between modified soil adjusted vegetation index (MSAVI) and salinity index (SI) based on the Landsat OLI image and field survey data and then proposed the salinization remote sensing information extraction model. However, only the linear relations between different feature space parameters has been considered in most previous relative studies, which has ignored the complicated impacts of biological and abiotic factors on salinization process [2], [29], [30].

Therefore, after fully considering the landscapes types of Yellow River Delta, five parameters that derived from Landsat 8 OLI images have been applied to establish ten monitoring indices based on four categories of feature space models for Yellow River Delta. Finally, the optimization detection model of soil salinization has been proposed.

II. MATERIALS AND METHODS

A. DATA COLLECTION AND PREPROCESSING

In this study, two kinds of data have been utilized to construct the models:(1) Satellite images;(2) field observed data. The Landsat 8 OLI data (Oct 26, 2016; 122/34) was used to retrieve the salinity index with spatio-temporall resolutions of 30m and 16 days, respectively. This above dataset can be obtained from USGS. The FLAASH models have been utilized to remove the influence of atmosphere and light on the reflection of ground objects [2], [7]. Figure 1 showed that 32 surface soil samples (30m×30m) with a depth of 0–10 cm were chosen from zones with diverse landscapes during Oct 25-26, 2016. Each sample was composed of five observed data with plum blossom shape. The 32 soil samples were crushed passed through a 2-mm mesh and then the suspensions of soil and water with 1:5 ratio were utilized to obtain the salt content [2], [14].

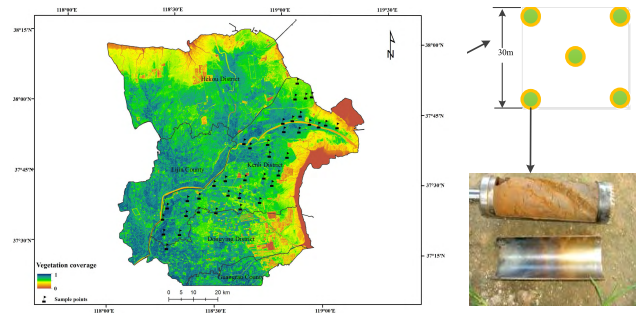


FIGURE 1. Spatial distribution of vegetation coverage and sample points in Yellow River Delta.

B. PRINCIPLE OF FEATURE SPACE (TAKING ALBEDO-MSAVI FEATURE SPACE AS EXAMPLE)

Previous studies showed that vegetation coverage would become become sparse with the deterioration of soil salinization [2], [10], [15], [22]. Therefore, the MSAVI is a better indicator to reflect the salinization process, especially in the arid and semi-arid zones [2], [4]. Surface albedo (Albedo) is an important parameter to indicate the short wave radiation

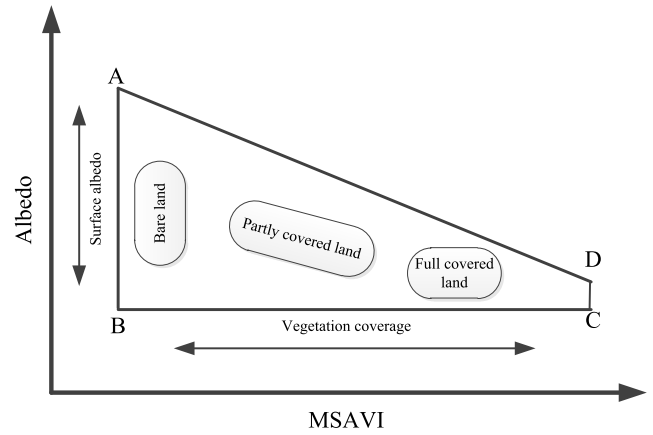


FIGURE 2. Principle of Albedo-MSAVI feature space.

from the earth’s surface to the sun. Its value would be greatly influenced by the soil surface conditions [2], [11], [17]. With the aggravation of salinization, the surface albedo increased correspondingly. As shown in Figure 2, there was a negative correlation between Albedo and MSAVI. The upper boundary A–D can reflects the severe salinization condition, which is the maximum Albedo corresponding [7], [19]. The lower boundary B–C represents the low Albedo line and it can reflects the slight salinization condition [2].

C. INDEX OF THE FEATURE SPACE MODEL

Albedo can reflect the short wave radiation from the land surface [2], [11], [15], [23], [31]–[33]. The vegetation growth and albedo can be indirectly affected by the soil salinization process. Thus, both albedo and vegetation indices (such as MSAVI) are better surface parameters to monitor the soil salinity [2], [15]. Salt in seawater is another dominant factor of soil salinity. Salinity index (SI) can directly reflect the salinization condition. Wetness index (WI) has significant negative effects on soil salinization [2], [7], [15], [27]. The soil salinization process will not only affect the vegetation growth, but also affect chemical substances contained in the soil. Therefore, the iron oxide index (I_{Fe2O3}) is also a better indicator for the soil salinization process [2], [9]. The five indices that derived from Landsat 8 OLI image, including Albedo, WI, MSAVI, SI, and I_{Fe2O3} are calculated as follows [2], [9], [11], [15]

$$\text{Albedo} = 0.356 \times \text{Blue} + 0.130 \times \text{Red} + 0.373 \times \text{Nir} + 0.085 \times \text{SW1} + 0.072 \times \text{SW2} - 0.0018 \quad (1)$$

$$\text{WI} = 0.1446 \times \text{Blue} + 0.1761 \times \text{Green} + 0.3322 \times \text{Red} + 0.3396 \times \text{Nir} - 0.6210 \times \text{SW1} - 0.4186 \times \text{SW2} \quad (2)$$

$$\text{MSAVI} = (2\text{Nir} + 1 - \sqrt{(2\text{Nir} + 1)^2 - 8(\text{Nir} - \text{Red})}) / 2 \quad (3)$$

$$\text{SI} = \sqrt{\text{Blue} \times \text{Red}} \quad (4)$$

$$I_{Fe2O3} = \frac{\text{Red}}{\text{Nir}} \quad (5)$$

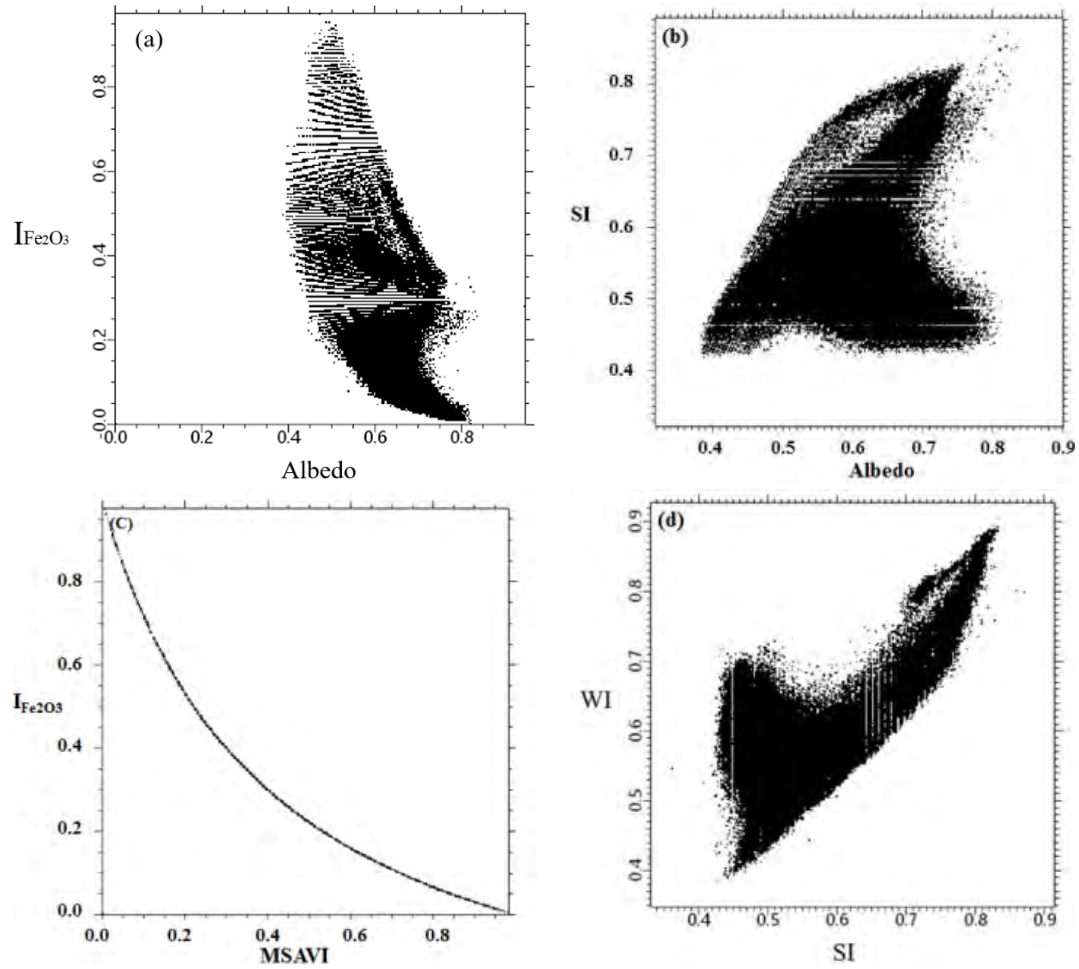


FIGURE 3. Four typical feature spaces models (a) $I_{Fe_2O_3}$ -Albedo; (b) Albedo-SI; (c) $I_{Fe_2O_3}$ -MSAVI; (d) WI-SI.

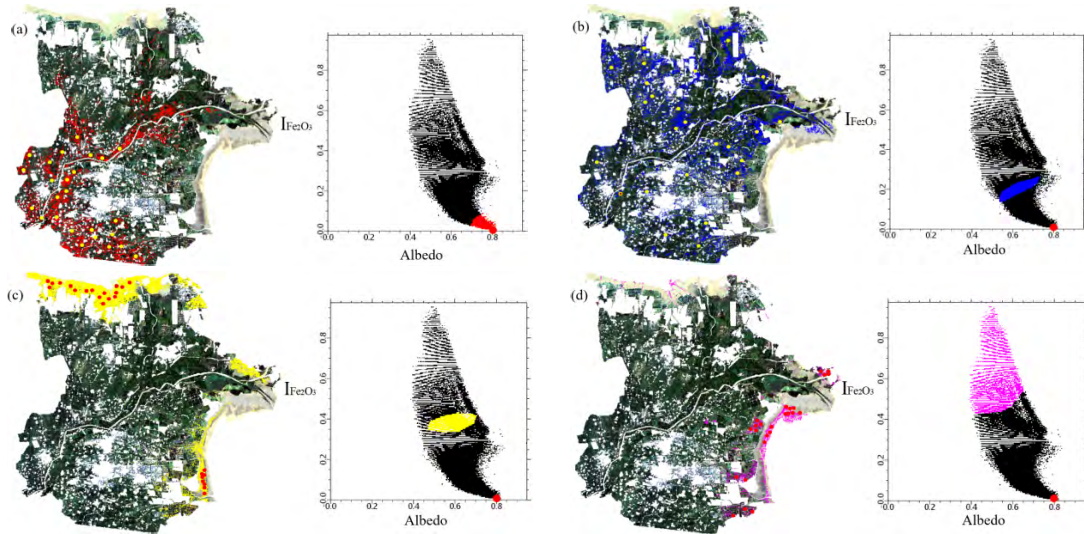


FIGURE 4. Salinization process in Albedo- $I_{Fe_2O_3}$ feature space (a) non; (b) mild; (c) moderate; (d) severe.

where Blue, Green, Red, Nir, SW_1 , and SW_2 are the reflectance of blue band, green band, red band, mid-infrared band, and near-infrared band, respectively.

D. INDEX STANDARDIZATION

There existed great difference among parameters, and the data standardization should be conducted to eliminate these

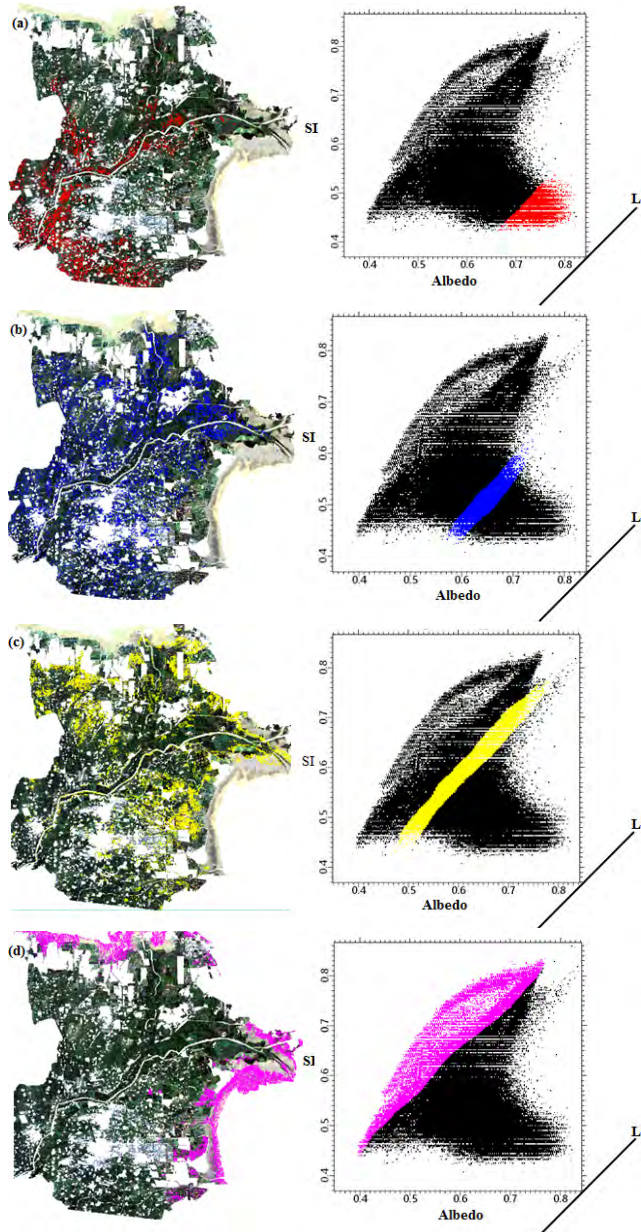


FIGURE 5. Salinization process in Albedo-SI feature space (a) non; (b) mild; (c) moderate; (d) severe.

differences [7], [11], [15], [34], [35]:

$$A = \frac{Al - Al_{\min}}{Al_{\max} - Al_{\min}} \quad (6)$$

where A refers to the standardized surface albedo index; Al refers to the surface albedo index; Al_{\min} and Al_{\max} refer to the minimum and maximum value of surface albedo index, respectively.

$$W = \frac{WI - WI_{\min}}{WI_{\max} - WI_{\min}} \quad (7)$$

where W refers to the standardized wetness index; WI refers to the wetness index; WI_{\min} and WI_{\max} refer to the minimum

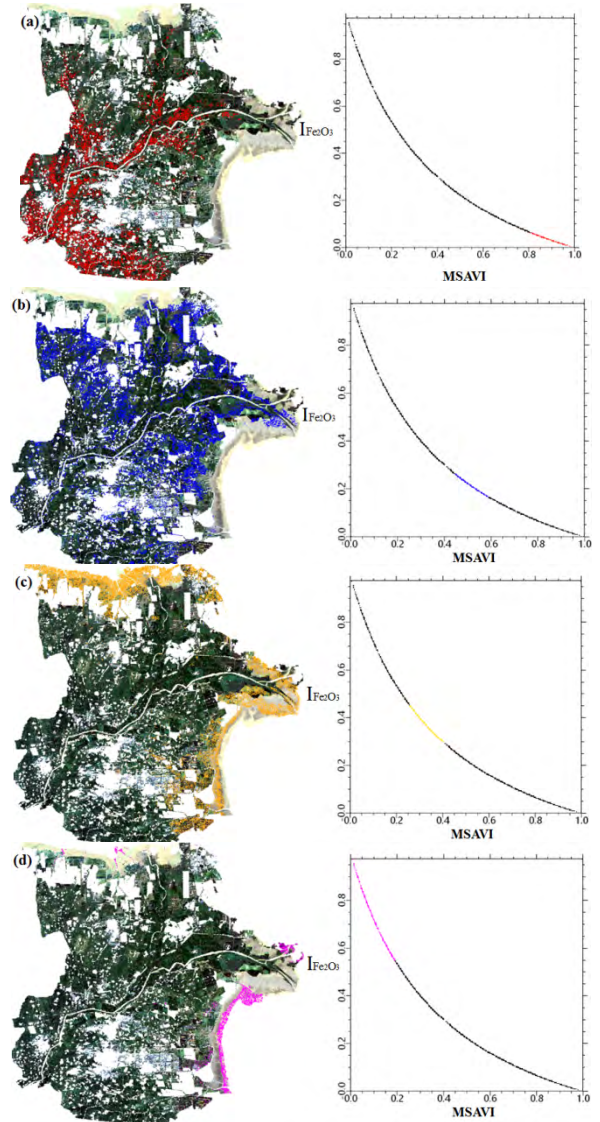


FIGURE 6. Salinization process in $I_{Fe_2O_3}$ -MSAVI feature space (a) non; (b) mild; (c) moderate; (d) severe.

and maximum value of wetness index, respectively.

$$M = \frac{VI - VI_{\min}}{VI_{\max} - VI_{\min}} \quad (8)$$

where M refers to the standardized vegetation index; VI is the vegetation index; VI_{\min} and VI_{\max} refer to the minimum and maximum value, respectively.

$$S = \frac{Si - Si_{\min}}{Si_{\max} - Si_{\min}} \quad (9)$$

where S refers to the standardized salinity index of i ; Si refers to the salinity index; Si_{\min} and Si_{\max} refer to the minimum and maximum value of salinity index, respectively.

$$I = \frac{I_{Fe_2O_3} - I_{Fe_2O_3 \min}}{I_{Fe_2O_3 \max} - I_{Fe_2O_3 \min}} \quad (10)$$

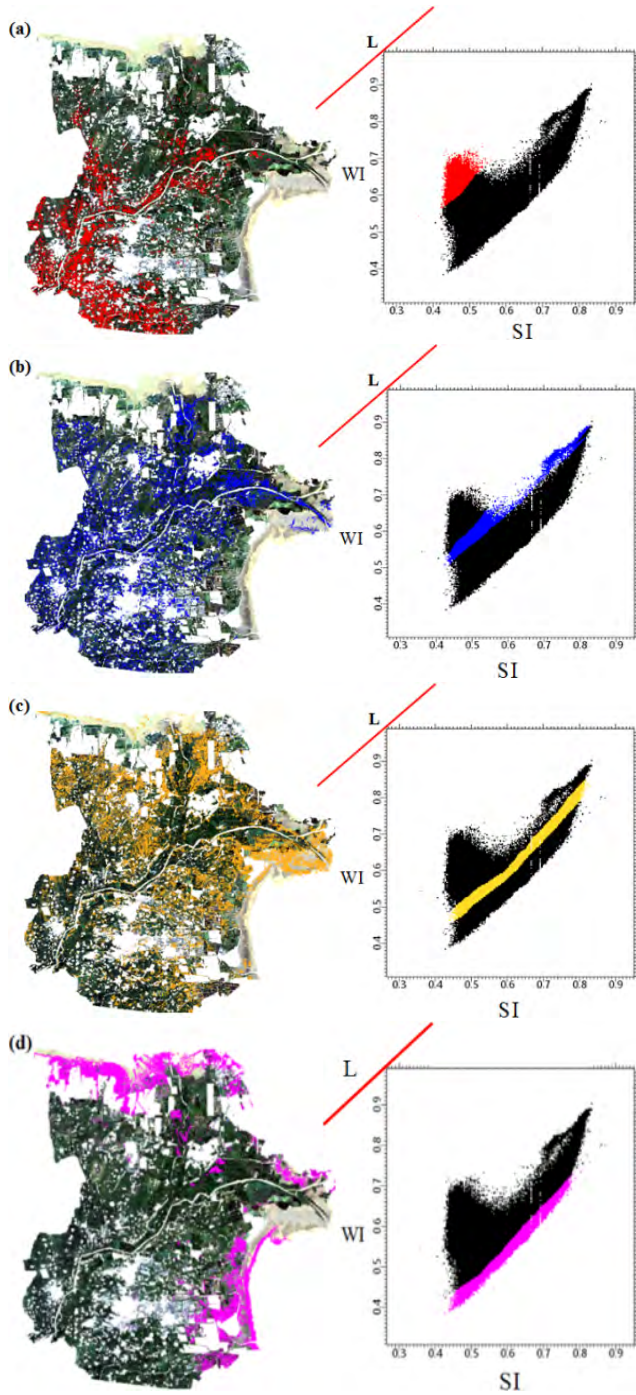


FIGURE 7. Salinization process in WI-SI feature space (a) non; (b) mild; (c) moderate; (d) severe.

where I is the standardized iron oxide index; $I_{Fe_2O_3}$ is the iron oxide index; $I_{Fe_2O_3min}$ and $I_{Fe_2O_3max}$ are the minimum and maximum value, respectively.

III. EXPERIMENTAL RESULTS AND ANALYSIS

A. CONSTRUCTION OF FEATURE SPACES

The zones with water and artificial impervious surface were extracted firstly with ENVI 5.3 [2]. Then, five indexes

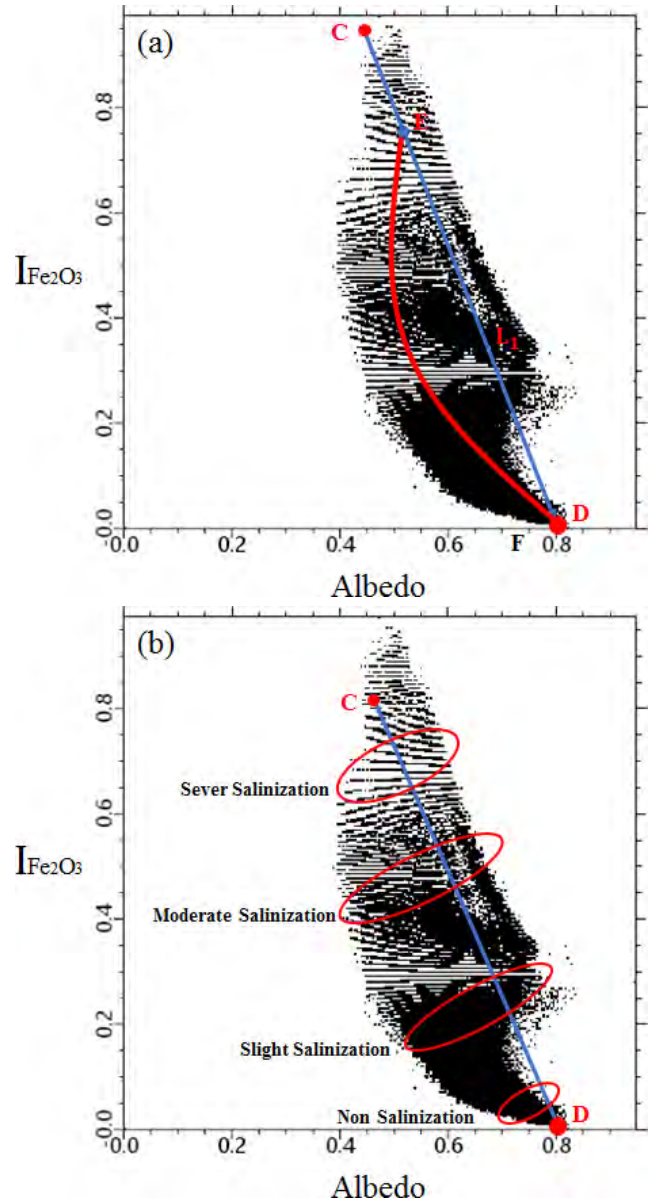


FIGURE 8. Salinization detection index model (SDI_1) based on Albedo- $I_{Fe_2O_3}$ feature space (a) Principle of SDI_1 (b) Levels of soil salinization in feature space.

including Albedo, MSAVI, SI, WI, and $I_{Fe_2O_3}$ were applied to establish ten feature spaces. According to the spatial change patterns of soil salinization process in feature space, ten feature spaces could be divided into four categories: (1) point to point feature space, includes Albedo- $I_{Fe_2O_3}$, Albedo-MSAVI, Albedo-WI, $I_{Fe_2O_3}$ -SI, $I_{Fe_2O_3}$ -WI, MSAVI-SI, MSAVI-WI; (2) point to line (wet line) feature space, includes Albedo-SI; (3) linear feature space, includes $I_{Fe_2O_3}$ -MSAVI; (4) point to line (soil line) feature space, includes WI-SI. In this study, Albedo-SI, $I_{Fe_2O_3}$ -MSAVI, Albedo- $I_{Fe_2O_3}$ and WI-SI feature spaces were applied to explore each category of feature space, respectively (Figure 3).

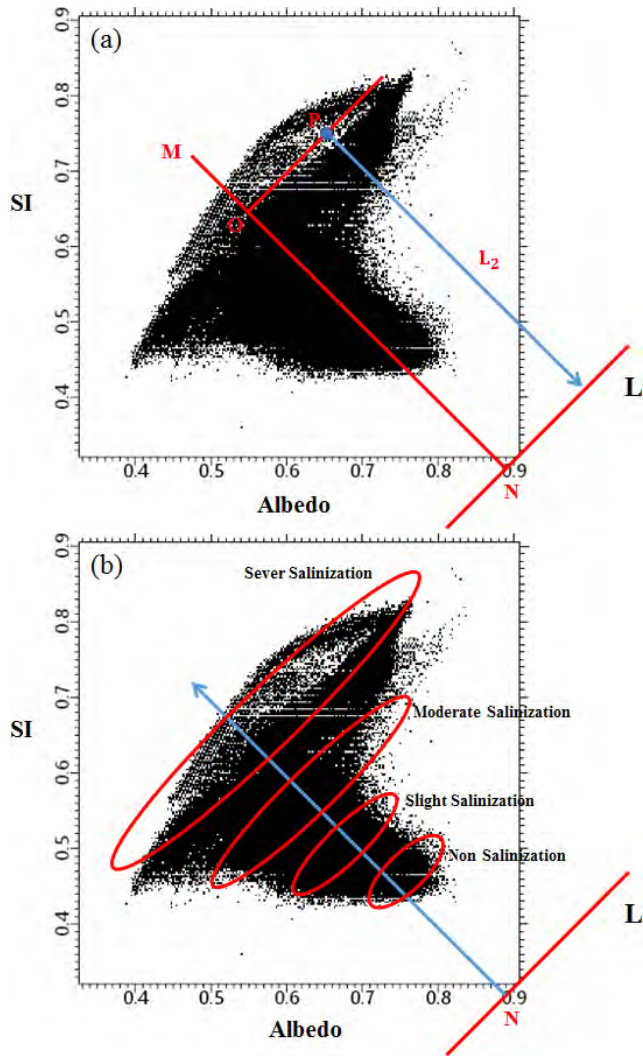


FIGURE 9. Salinization detection index model (SDI_2) based on Albedo-SI feature space (a) Principle of SDI_2 (b) Levels of soil salinization in feature space.

B. SPATIAL DISTRIBUTION SALINIZATION MODELS

As was shown in Figure 4, we chose four point clusters to indicate different levels of soil salinization according to the distance to the point (0.8, 0) in Albedo- I_{Fe2O3} feature space. The results showed that the spatial distributions of different categories of soil salinization (non salinization, mild salinization, moderate salinization, and severe salinization) differed greatly in the Albedo- I_{Fe2O3} feature space.

Figure 5 showed that the distance to the L line that is parallel to the “wet line” could be utilized to reflect the soil salinization process in Albedo-SI feature space. The soil salinization condition would become more severe with the increasing distance that from the L-line [2].

As was shown in Figure 6, this fit curve could better reflect the change process of soil salinization in I_{Fe2O3} -MSAVI feature space. These spatial distribution laws could help to distinguish levels of soil salinization.

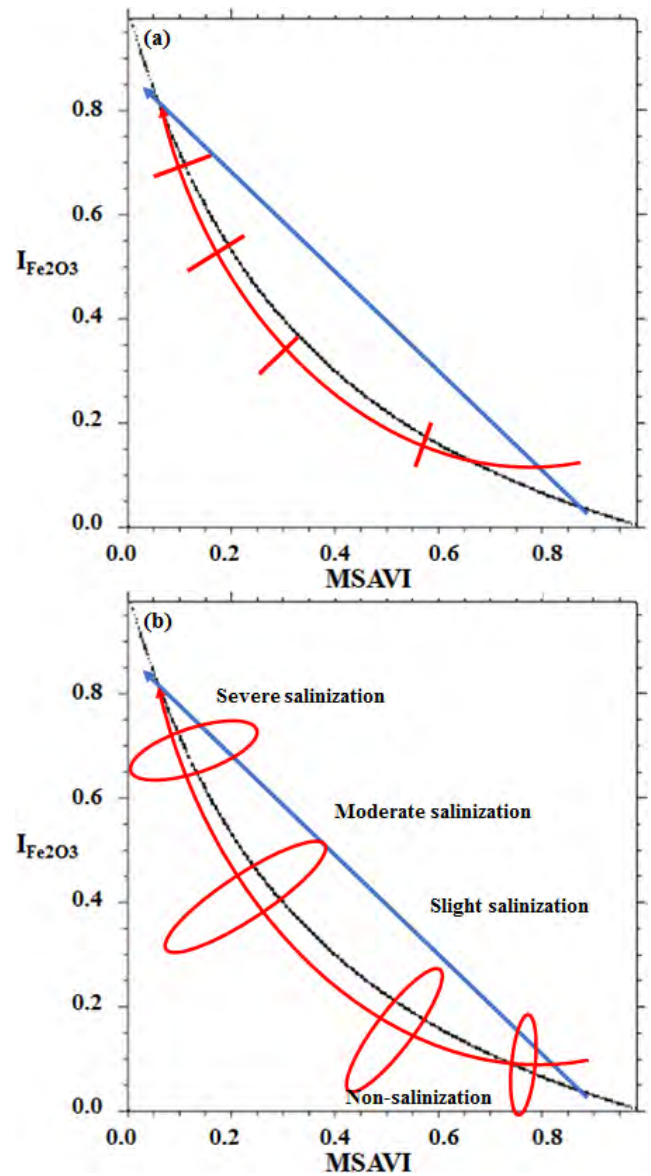


FIGURE 10. Salinization detection index model (SDI_3) based on I_{Fe2O3} -MSAVI feature space (a) Principle of SDI_3 (b) Levels of soil salinization in feature space.

Similar to Figure 7, the distance from any point to L line that was parallel to the soil line could better reflect the degrees of salinization condition in Albedo-SI feature space. The salinization would be more severe when the distance from the L-line became larger [2].

As was shown in Figure 8, the distance to D (0.8, 0) could better explain the soil salinization process in Albedo- I_{Fe2O3} feature space. The further away any point from point D, the more severe soil salinization. The salinization detection function (SDI_1) was developed as follows:

$$SDI1 = L_1 = \sqrt{(Albedo - 0.8)^2 + I_{Fe2O3}^2} \quad (11)$$

As shown in Figure 9, the distance to L line could indicate the soil salinization process in Albedo-SI feature space. The further away from the L line, the more severe soil salinization.

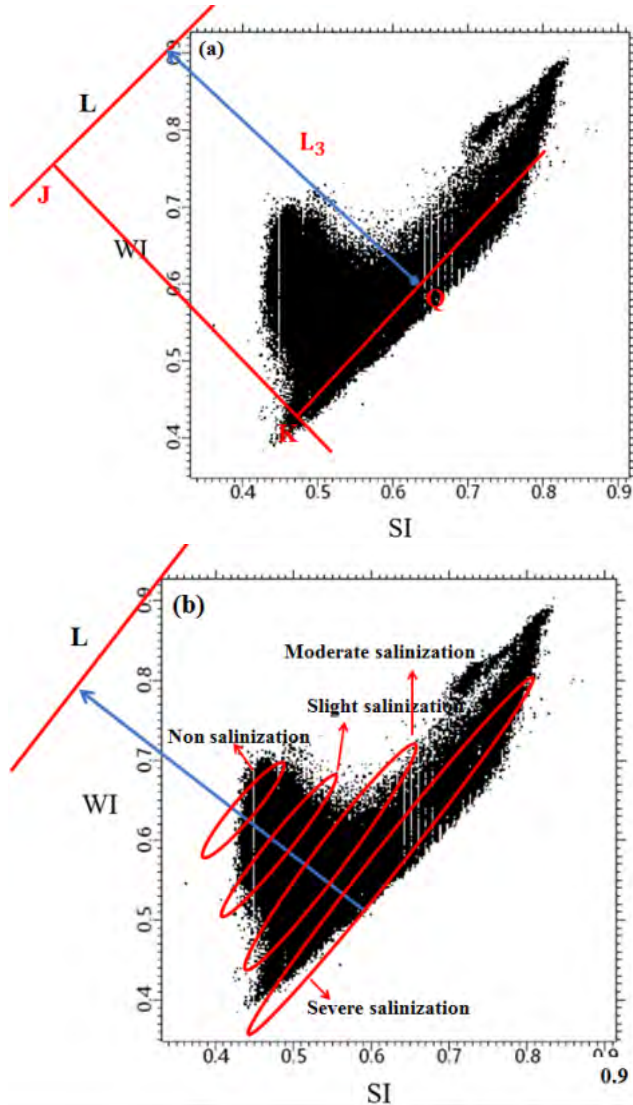


FIGURE 11. Salinization detection index model (SDI_4) based on WI-SI feature space (a) Principle of SDI_4 (b) Levels of soil salinization in feature space.

The salinization monitoring function (SDI_2) was proposed and M referred to the slope of “wet line”:

$$SDI_2 = L_2 = \frac{|1 + M \times Albedo - SI|}{\sqrt{1 + M^2}} \quad (12)$$

Figure 10 showed that the I_{Fe2O3} -MSAVI feature space was divided into different parts in the vertical direction of the curve, which could reflect the salinization process. And then different levels of soil salinization could be better distinguished. The region perpendicular to the I_{Fe2O3} -MSAVI feature space can be determined by a binary linear function considering the linear relationship between the above factors.

$$SDI_3 = L_3 = a \times I_{Fe2O3} - MSAVI \quad (13)$$

where a refers to the slope of the linear equation.

Similar to Figure 11, the distance to L line could be utilized to distinguish different levels of soil salinization in WI-SI feature space. The soil salinization would become more severe

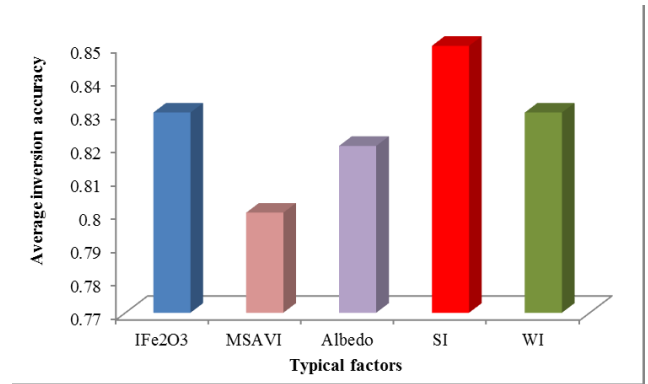


FIGURE 12. Average inversion accuracy of each typical factor.

with the increasing distance to the L line (parallel to the soil line). The salinization monitoring function of soil salinization (SDI_4) was established.

$$SDI_4 = L_4 = \frac{|SI - pWI - 1|}{\sqrt{1 + p^2}} \quad (14)$$

where p is the slope of “soil line”.

IV. RESULTS AND DISCUSSIONS

Ten salinization detection indices were obtained utilized the above four categories of models, then the inversion accuracies have been analyzed and compared based on 32 field observation samples([2], Table 1 and Figure 1). The results (Table 2) showed that WI-SI point to line (soil line) model had the largest inversion accuracy with $R^2 = 0.88$, followed by Albedo-SI point to line (wet line) model ($R^2 = 0.87$) and Albedo- I_{Fe2O3} point to point model ($R^2 = 0.86$). On the contrary, the Albedo-MSAVI point to point model had the smallest inversion accuracy with $R^2 = 0.77$. This result was consistent with that of Wang *et al.* [10] and Guo *et al.* [34]. The reasons lied in the fact that the point to line (wet line or soil line) models had fully considered the non-linear relations among different variables. It could better eliminate the effects of soil background or vegetation saturation effect [2], [35]–[38]. As shown in Figure 12, the average precision of feature space models that contained SI was the best with $R^2 = 0.85$, followed by that of I_{Fe2O3} ($R^2 = 0.83$) and WI ($R^2 = 0.83$). On the contrary, the average precision of feature space model that contained MSAVI was the worst with $R^2 = 0.80$. This above conclusions were consistent with the studies of Ivushkin *et al.* [3] and Guo and Wen [7]. The reason was that the salinity would precipitate out of the surface soil, which apparently affected the surface albedo [2], [34], [32]–[36]. Moreover, iron oxide was an important factor that affected the spectral characteristics of the soil [9]. Many absorption characteristics of soil in the visible band had significant relations with iron oxides. And the reflectivity of soil would decrease with the presence of iron oxides [2], [9], [40]. Moreover, the chemical weathering played an important role in the soil salinization process [2], [41]. Humidity index derives from the third component of Hat Transformation with Landsat8 OLI images, which can better reflects the condition

TABLE 1. Values of field observed soil salt content

Sample number	Filed observed salt content/ $\text{g}\cdot\text{kg}^{-1}$	Sample number	Filed observed salt content/ $\text{g}\cdot\text{kg}^{-1}$
S01	3.07	S17	3.97
S02	5.01	S18	1.51
S03	4.03	S19	1.22
S04	1.59	S20	1.22
S05	2.72	S21	1.20
S06	2.82	S22	1.12
S07	3.38	S23	1.89
S08	3.23	S24	1.49
S09	3.12	S25	1.84
S10	2.09	S26	1.41
S11	2.32	S27	1.35
S12	2.14	S28	2.10
S13	1.99	S29	2.56
S14	1.74	S30	1.89
S15	1.72	S31	1.65
S16	2.65	S32	1.47

TABLE 2. Precision comparisons among different detection models.

Category of model	Feature space	R^2
Point to point model	Albedo- $I_{\text{Fe}2\text{O}3}$	0.86
	Albedo-MSAVI	0.77
	Albedo-WI	0.80
	$I_{\text{Fe}2\text{O}3}$ -SI	0.85
	$I_{\text{Fe}2\text{O}3}$ -WI	0.80
	MSAVI-SI	0.81
Point to line (wet line)model	MSAVI-WI	0.84
	Albedo-SI	0.87
Linear model	$I_{\text{Fe}2\text{O}3}$ -MSAVI	0.81
Point to line (soil line)model	WI-SI	0.88

of soil humidity in the study area [2], [34], [42]. There existed better relations between soil moisture and soil salinization process[42]. Salt in seawater was another dominant factor of soil salinity [2]. Soil humidity would be significantly affected by seawater, so that the soil salinization occurred commonly in the study area [27], [42]. Although, MSAVI could better reflect the vegetation condition, there were many types of salt-tolerant plants. And vegetation coverage was not the smallest in some region with severe salinization [2], [15], [41], [43]. Therefore, the MSAVI was not the optimal indices to reflect the condition of soil salinization for this study area. In conclusion, three typical surface parameters, including SI, $I_{\text{Fe}2\text{O}3}$, and WI were better indices to retrieve the salinization information. And for the Yellow River Delta, the WI-SI point to line (soil line) model, the Albedo-SI point to line (wet line) model and the Albedo- $I_{\text{Fe}2\text{O}3}$ point to point model have better applicability to detect the salinization conditions.

V. CONCLUSION

In this paper, five inversed parameters that derived from Landsat 8 OLI image, including MSAVI, Albedo, WI, $I_{\text{Fe}2\text{O}3}$, and SI have been applied to construct ten feature spaces. And then four categories of models have been established. After analysis and comparison, three typical surface parameters, including SI ($R^2 = 0.85$), $I_{\text{Fe}2\text{O}3}$ ($R^2 = 0.83$), and WI ($R^2 = 0.83$) are better indices to retrieve the salinization information and the WI-SI point to line (soil line) model ($R^2 = 0.88$), the Albedo-SI point to line (wet line) model ($R^2 = 0.87$) and the Albedo- $I_{\text{Fe}2\text{O}3}$ point to point model ($R^2 = 0.86$) have better applicability to monitor the salinization condition in Yellow River Delta. However, further research is needed to clarify the comprehensive and interaction effects of different factors (climate and human activities) on soil salinization process.

REFERENCES

- [1] A. Allbed and L. Kumar, "Soil salinity mapping and monitoring in arid and semi-arid regions using remote sensing technology: A review," *Adv. Remote Sens.*, vol. 2, no. 4, pp. 373–385, 2013.
- [2] B. Guo, W. Zang, W. Luo, Y. Wen, F. Yang, B. Han, Y. Fan, X. Chen, Z. Qi, Z. Wang, S. Chen, and X. Yang, "Detection model of soil salinization information in the Yellow River Delta based on feature space models with typical surface parameters derived from Landsat8 OLI image," *Geomatics, Natural Hazards Risk*, vol. 11, no. 1, pp. 288–300, Jan. 2020.
- [3] K. Ivushkin, H. Bartholomeus, A. K. Bregt, A. Pulatov, B. Kempen, and L. de Sousa, "Global mapping of soil salinity change," *Remote Sens. Environ.*, vol. 231, Sep. 2019, Art. no. 111260.
- [4] X. P. Ha, J. L. Ding, T. Puxifulati, J. Y. Luo, and F. Zhang, "Research on extraction of salinized soil information in arid areas based on SI-Albedo characteristic space-taking the Keriya river basin Oasis as an example," *Acta Pedologica Sin.*, vol. 46, no. 3, pp. 381–390, May 2009.
- [5] S. Thiam, G. B. Villamor, N. Kyei-Baffour, and F. Matty, "Soil salinity assessment and coping strategies in the coastal agricultural landscape in Djilor district, Senegal," *Land Use Policy*, vol. 88, Nov. 2019, Art. no. 104191.
- [6] N. M. Khan, V. V. Rastokuev, Y. Sato, and S. Shiozawa, "Assessment of hydrosaline land degradation by using a simple approach of remote sensing indicators," *Agricult. Water Manage.*, vol. 77, nos. 1–3, pp. 96–109, Aug. 2005.
- [7] B. Guo and Y. Wen, "An optimal monitoring model of desertification in Naiman Banner based on feature space utilizing Landsat8 OLI image," *IEEE Access*, vol. 8, pp. 4761–4768, Jan. 2020.
- [8] D. Ren, B. Wei, X. Xu, B. Engel, G. Li, Q. Huang, Y. Xiong, and G. Huang, "Analyzing spatiotemporal characteristics of soil salinity in arid irrigated agro-ecosystems using integrated approaches," *Geoderma*, vol. 356, Dec. 2019, Art. no. 113935.
- [9] J. Peng, H. Y. Xiang, Q. Zhou, Y. Z. Zhang, J. Q. Wang, and X. A. Peng, "Hyperspectral response of soil iron oxide," *Spectrosc. Spectr. Anal.*, vol. 33, no. 2, pp. 502–506, Jul. 2013.
- [10] F. Wang, J. L. Ding, and M. C. Wu, "Remote sensing model of soil salinization based on NDVI-SI characteristic space," *Trans. CSAE*, vol. 26, no. 8, pp. 168–173, Aug. 2010.
- [11] Y. N. Zeng, N. P. Xiang, Z. D. Feng, and H. Xu, "Albedo-NDVI space and remote sensing synthesis index models for desertification monitoring," *Scientia Geographica Sinica*, vol. 26, no. 1, pp. 75–82, Feb. 2006.
- [12] G. I. Metternicht and J. A. Zinck, "Remote sensing of soil salinity: Potentials and constraints," *Remote Sens. Environ.*, vol. 85, no. 1, pp. 1–20, Apr. 2003.
- [13] Y. Liu, F. Zhang, C. Wang, S. Wu, J. Liu, A. Xu, K. Pan, and X. Pan, "Estimating the soil salinity over partially vegetated surfaces from multi-spectral remote sensing image using non-negative matrix factorization," *Geoderma*, vol. 354, Nov. 2019, Art. no. 113887.
- [14] Y. F. Sun, "Study on soil salinization dynamics in Yinchuan plain based on remote sensing monitoring index model," *Underground Water*, vol. 41, no. 5, pp. 80–82, Sep. 2019.

- [15] Y. H. Li, J. L. Ding, Y. M. Sun, G. Wang, and L. Wang, "Remote sensing monitoring models of soil salinization based on the three dimensional feature space of MSAVI-WI-SI," *Res. Soil Water Conservation*, vol. 22, no. 4, pp. 113–117 and 121, Aug. 2015.
- [16] L. Lei, H. N. Jiang, A. Ke, and M. C. Wu, "Analysis and extraction of saline soil hyperspectral remote sensing information for arid area," *J. Arid Land Resource Environ.*, vol. 28, no. 3, pp. 112–118, Mar. 2014.
- [17] Y. Yao, J. L. Ding, F. Zhang, G. Wang, and H. N. Jiang, "Monitoring of soil salinization in Northern Tarim Basin, Xinjiang of China in dry and wet seasons based on remote sensing," *Chin. J. Appl. Ecol.*, vol. 24, no. 11, pp. 3213–3220, Nov. 2013.
- [18] T. Du, J. Z. Jiao, Y. W. Jie, and J. Zhang, "Method exploration for quantitative evaluation of salinization using Landsat satellite image: A case study of Guazhou-Dunhuang area," *Hubei Agricult. Sci.*, vol. 57, no. 1, pp. 51–55, Jan. 2018.
- [19] R. Wang, Z. H. Liu, C. Z. Li, and R. J. Wang, "Remote sensing interpretation signs and imaging characteristics of land salinity, desertification in the Hami basin," *Xinjiang Agricult. Sci.*, vol. 49, no. 5, pp. 950–953, May 2012.
- [20] B. Z. He, J. L. Ding, B. H. Liu, and J. Z. Wang, "Spatiotemporal variation of soil salinization in Weigan-Kuqa river delta Oasis," *Sci. Silvae Sinica*, vol. 55, no. 9, pp. 185–196, Sep. 2019.
- [21] X. Wang, Q. M. Liu, Z. Y. Qu, L. P. Wang, X. J. Li, and Y. Q. Wang, "Inversion and verification of salinity soil moisture using microwave radar," *Trans. Chin. Soc. Agricult. Eng.*, vol. 33, no. 11, pp. 108–114, Jun. 2017.
- [22] T. Y. Zhang, L. Wang, C. Luo, and L. Peng, "Spatiotemporal change of soil salinization in Manasi river basin," *Res. Soil Water Conservation*, vol. 23, no. 1, pp. 228–233, Dec. 2015.
- [23] E. Scudiero, T. H. Skaggs, and D. L. Corwin, "Regional-scale soil salinity assessment using Landsat ETM + canopy reflectance," *Remote Sens. Environ.*, vol. 169, pp. 335–343, Nov. 2015.
- [24] J. Wang, J. Ding, D. Yu, D. Teng, B. He, X. Chen, X. Ge, Z. Zhang, Y. Wang, X. Yang, T. Shi, and F. Su, "Machine learning-based detection of soil salinity in an arid desert region, Northwest China: A comparison between Landsat-8 OLI and Sentinel-2 MSI," *Sci. Total Environ.*, vol. 707, Mar. 2020, Art. no. 136092.
- [25] A. Abuelgasim and R. Ammad, "Mapping soil salinity in arid and semi-arid regions using Landsat 8 OLI satellite data," *Remote Sens. Appl., Soc. Environ.*, vol. 13, pp. 415–425, Jan. 2019.
- [26] Z. K. Curtis, H. Liao, S. Li, P. V. Sampath, and D. P. Lusch, "A multiscale assessment of shallow groundwater salinization in Michigan," *Groundwater*, vol. 57, no. 5, pp. 784–806, Sep. 2019.
- [27] J. L. Ding, Y. Yao, and F. Wang, "Detecting soil salinization in arid regions using spectral feature space derived from remote sensing data," *Acta Ecologica Sinica*, vol. 34, no. 16, pp. 4620–4631, Mar. 2014.
- [28] T. Y. Zhang, L. Wang, P. L. Zeng, T. Wang, Y. H. Geng, and H. Wang, "Soil salinization in the irrigated area of the Manas River basin based on MSAVI-SI feature space," *Arid Zone Res.*, vol. 33, no. 3, pp. 499–505, May 2016.
- [29] M. Babutzka, J. Mietz, and A. Burkert, "Investigation of the salinization of steel surfaces in marine environment," *Mater. Corrosion*, vol. 70, no. 6, pp. 1016–1025, Jun. 2019.
- [30] A. Singh, "Managing the salinization and drainage problems of irrigated areas through remote sensing and GIS techniques," *Ecol. Indicators*, vol. 89, pp. 584–589, Jun. 2018.
- [31] M. A. E. AbdelRahman, M. M. Metwaly, and A. Shalaby, "Quantitative assessment of soil saline degradation using remote sensing indices in Siwa Oasis," *Remote Sens. Appl., Soc. Environ.*, vol. 13, pp. 53–60, Jan. 2019.
- [32] E. Asfaw, K. V. Suryabagavan, and M. Argaw, "Soil salinity modeling and mapping using remote sensing and GIS: The case of Wonji sugar cane irrigation farm, Ethiopia," *J. Saudi Soc. Agricult. Sci.*, vol. 17, no. 3, pp. 250–258, Jul. 2018.
- [33] T. Gorji, E. Sertel, and A. Tanik, "Monitoring soil salinity via remote sensing technology under data scarce conditions: A case study from Turkey," *Ecol. Indicators*, vol. 74, pp. 384–391, Mar. 2017.
- [34] B. Guo, B. Han, F. Yang, Y. Fan, L. Jiang, S. Chen, W. Yang, R. Gong, and T. Liang, "Salinization information extraction model based on VI-SI feature space combinations in the Yellow River Delta based on Landsat 8 OLI image," *Geomatics, Natural Hazards Risk*, vol. 10, no. 1, pp. 1863–1878, Jan. 2019.
- [35] K. M. Guo, and K. L. Jia, "Remote sensing monitoring research on soil salinization based on hyperspectral index: Taking Pingluo county as an example," *Ningxia Eng. Technol.*, vol. 18, no. 1, pp. 91–96, Mar. 2019.
- [36] X. L. Feng and Q. M. Liu, "Regional soil salinity monitoring based on multi-source collaborative remote sensing data," *Trans. Chin. Soc. Agricult. Mach.*, vol. 49, no. 7, pp. 127–133, May 2018.
- [37] T. Y. Zhang, L. Wang, H. Wang, L. Peng, and C. Luo, "Assessment of soil salinization ecological environment change in the Manas river basin using remote sensing technology," *Acta Ecologica Sinica*, vol. 37, no. 9, pp. 3009–3018, 2017.
- [38] Z. Yan, J. L. Ding, Z. Y. Niu, and Y. H. Li, "Soil salinization monitoring in the Ebinur lake region at a field scale based on GF-1 image," *J. Desert Res.*, vol. 36, no. 4, pp. 1070–1078, Jul. 2017.
- [39] I. Gulnur, N. Ilyas, and S. S. Duan, "The extraction of saline soil information in typical Oasis of arid area using fully polarimetric Radarsat-2 data," *China Rural Water Hydropower*, vol. 12, pp. 13–19, Dec. 2018.
- [40] B. Guo, F. Yang, B. Han, Y. Fan, S. Chen, W. Yang, and L. Jiang, "A model for the rapid monitoring of soil salinization in the Yellow River Delta using Landsat 8 OLI imagery based on VI-SI feature space," *Remote Sens. Lett.*, vol. 10, no. 8, pp. 796–805, Aug. 2019.
- [41] B. Guo, F. Yang, Y. Fan, B. Han, S. Chen, and W. Yang, "Dynamic monitoring of soil salinization in Yellow River delta utilizing MSAVI-SI feature space models with Landsat images," *Environ. Earth Sci.*, vol. 78, no. 10, p. 308, May 2019.
- [42] Z. Y. Niu, J. L. Ding, Y. H. Li, S. Wang, L. Wang, and C. X. Ma, "Soil salinization information extraction method based on GF-1 image," *Arid Land Geography*, vol. 39, no. 1, pp. 171–181, Jan. 2016.
- [43] Q. M. Liu, Q. M. Cheng, X. Wang, and X. J. Li, "Soil salinity inversion in Hetao irrigation district using microwave radar," *Trans. Chin. Soc. Agricult. Eng.*, vol. 32, no. 16, pp. 109–114, Aug. 2016.



BING GUO was born in Zibo, Shandong, in 1987. He received the B.S. degree in geographic information system from Ludong University, Yantai, in 2010, and the M.S. and Ph.D. degrees in cartography and geographical information system from the University of Chinese Academy of Sciences, Beijing, in 2013 and 2016, respectively.

From 2016 to 2019, he was a Lecturer with the School of Civil Architectural Engineering, Shandong University of Technology. He is the author of one book and more than 50 articles. His research interests include remote sensing, ecological environment, natural hazards, global change, and land use change.

Dr. Guo was a member of the Member of Chinese Geographical Society and was a recipient of the Dean Excellence Award of University of Chinese Academy of Sciences and the Excellent Thesis Award of Journal of Arid land, in 2018.



WENQIAN ZANG was born in Xinxiang, Henan, in 1984. He received the B.S. and M.S degrees in resources environment and the management of urban and rural planning from Henan Polytechnic University, Jiaozuo, in 2006, and the Ph.D. degree in geography from the University of Chinese Academy of Sciences, Beijing, in 2013.

From 2013 to 2019, he was an Assistant Professor with the Institute of Remote Sensing and Digital Earth, Chinese Academy of Sciences. He is the author of more than 20 articles and two Chinese National Invention Patents. His research interests include remote sensing image processing, cluster computing, and natural hazards.

Dr. Zang was a member of the China Association of Remote Sensing Application and won the first prize of science and technology progress award of Xinjiang Uygur Autonomous Region, in 2017.



RUI ZHANG received the Ph.D. degree in cartography and geography information system from the Institute of Remote Sensing and Digital Earth (RADI), in 2019. His scientific interests are in the fields of land use classification, remote sensing monitoring of disaster environment based on machine learning, and spatial information science including remote sensing, GIS, and their integration.

...